Hydrophobicity in a simple model of water: solvation and hydrogen bond energies

K.A.T. Silverstein[†] and K.A. Dill[a]

Department of Pharmaceutical Chemistry and [†]Graduate Group in Biophysics,

University of California, San Francisco CA 94143-1204 USA

A.D.J. Haymet[a]

School of Chemistry, University of Sydney, NSW 2006 Australia

Presented at the 13th Symposium on Thermophysical Properties, Boulder, CO USA

22-27 June 1997

[a]Authors to whom correspondence should be addressed

Keywords: hydrophobicity, phase diagram, two dimensions, water model

ABSTRACT

We explore a simple model of water: Lennard-Jones disks in 2 dimensions, subject to a Gaussian orientation-dependent hydrogen-bond function. The model, originally developed by Ben-Naim, shows the anomalous features of water and aspects of the hydrophobic effect. Here we further explore its phase diagram and related properties by NPT Monte Carlo simulations.

INTRODUCTION

We explore the properties of a simple model of water, proposed originally by Ben-Naim[1]. We have found, through NPT Monte Carlo simulations, that this model qualitatively reproduces several anomalous trends of water, including the density anomaly, a negative thermal expansion coefficient at low temperature, the large heat capacity of the condensed phase, a minimum in the isothermal compressibility as a function of temperature, and the proper temperature trends of the thermodynamics of hydrophobic transfers[2].

The model, which we call MB water (because of its resemblance to the Mercedes-Benz logo) represents water molecules as standard Lennard-Jones disks in two dimensions with three symmetrically-arranged arms. The arms attract each other through an explicit hydrogen-bonding interaction. The hydrogen bond is defined to be optimal at a specified distance, and relative orientation of the two participating molecules (i.e., bonding arm pointing directly towards the center of the other molecule.) Deviations from this lowest-energy hydrogen bond are described by a Gaussian function with a single width parameter. All energies and temperatures are reported in reduced units, normalized to the strength of the optimal hydrogen bond, ϵ_{HB} (e.g., $T^* = k_B T/\epsilon_{HB}$, $H^* = H/\epsilon_{HB}$). Likewise all distances are scaled by the length of an idealized hydrogen bond separation, r_{HB} (e.g., $V^* = V/r_{HB}^2$). More details may be found in the original paper[1] and [2, 3]. We further explore some macroscopic and microscopic properties of MB water in the following two sections. An additional general comment on constant-pressure Monte Carlo simulations is made in the Appendix.

PHASE DIAGRAM

In addition to the properties mentioned above, MB water shows some other similarities to real water. We display a rough P-T phase diagram in Figure 1. The solid/liquid and solid/gas boundaries were determined by locating the large jump in the heat capacity when slowly raising the temperature from an initial ice configuration (with long equilibration times in between temperatures). The liquid/gas boundaries were determined from the method of Hansen and Verlet[4]. The most notable property of this sketch is the negative slope of the liquid-solid coexistence line. Water is among the few substances which have this property.

DETAILS OF HYDROGEN BONDING

Figure 2 shows the centers pair correlation function, $g(r)$, at several temperatures. The first shoulder occurs at the characteristic van der Waals distance of the model. The primary and subsequent peaks occur at the first, second, third, etc. hydrogen-bond neighbor distances. A pronounced breakdown in structure is observed with temperature.

Some insight into a possible molecular cause of the density anomaly may be obtained by tracking some other structural features. The density anomaly appears to arise from a two-part mechanism. Initially, ice has a very open hydrogen-bonded structure. Upon melting, however, some of these hydrogen bonds (HB) are weakened or broken, and replaced with more dense-packing van der Waals (VDW) interactions. This process of exchanging open HB arrangements for more-compact and higher-energetic VDW

interactions continues in the fluid until thermal fluctuations begin to drive the molecules apart once the temperature of maximum density (TMD) is passed (the TMD in this model occurs at T*=0.18).

Evidence supporting this explanation can be obtained by tracking the distributions of HB and VDW coordination of the water molecules. To do this, we assign an arbitrary energetic cutoff. If the HB or VDW energetic terms respectively are below the cutoff in a pairwise interaction, then each of the molecule's corresponding coordination counters is incremented. The cutoffs (-0.5 for HB, and -0.06 for the VDW), correspond to minima in the pair interaction energies. The minimum that corresponds to the HB cutoff is quite broad, and hence the trends in HB coordination are fairly insensitive to the cutoff value. The average HB coordination starts out quite high in the low-temperature fluid, and steadily decreases with temperature, as can be seen in Figure 3. In contrast, the minimum corresponding to the VDW cutoff is very sharp, and more lenient cutoffs can change the VDW counting considerably. This is partly because the very weakest VDW interactions overlap to some degree with corresponding h-bonding distances. Figure 4 shows that initially the number of strong VDW contacts increase and then levels off before decreasing. Weaker VDW contacts diminish after the TMD.

The exchange of HB and VDW contacts leads to restructuring in the fluid. Hence, the variance in the distribution of HB coordinations is quite high, peaking at the TMD (see Figure 5). This is consistent with Stillinger's explanation of the density anomaly[5], in which compression arises from the shift from ice-like six-membered h-bonded rings towards more and more strained h-bonded ring networks.

It is possible that the minimum in the compressibility arises from the same balance

of VDW and HB interactions. The initial increase in VDW contacts crowds the local molecular environment to some degree, making the fluid less compressible. Then, as the number of bent or broken h-bonds becomes appreciable, the fluid ultimately increases its compressibility.

The microscopic origins of the hydrophobic effect have long been under debate. One group[6, 7, 8, 9, 10] holds that hydrophobicity results mostly from the small size of the water molecule, and not from water structuring by the solute. Much of this argument may simply be semantic[11, 12, 13]. We believe that the large positive heat capacity of insertion of nonpolar solutes is the defining feature of hydrophobicity. The present model suggests water structuring gives rise to the heat capacity. At issue is whether the water molecules at the solute surface change their degree of ordering differently than bulk water molecules with temperature. Figure 6 and 7 show that they do.

We define the first-shell water molecules as those within a given cutoff-distance from the solute (taken to be the first minimum in the solute-water pair correlation function). At low temperature, the water-water pair correlation, $g_{WW}(r)$, for the first-shell water molecules is remarkably similar to that of bulk water, despite the presence of the nearby solute (see Figure 6). Only the VDW peak at a distance of ≈ 0.8 is diminished relative to the bulk counterpart. Then at higher temperature, the first hydrogen-bonding peak of the shell molecules becomes weaker than the corresponding bulk-water peak. The first and second neighbors, respectively, of bulk and shell water molecules are defined as those within the first and second minima of $g_{WW}(r)$. The angular distributions of water molecules in each of these categories are shown in Figure 7 at several temperatures. We find that at all temperatures studied, the first-neigbors of shell molecules have more

orientational order than those about bulk water molecules. Second-neighbors to shell water molecules only show enhanced ordering at lower temperatures.

CONCLUSIONS

In this work we have further evaluated the MB model of water, and have investigated finer structural rearrangements with increasing temperature. We find that MB water has the qualitatively correct of the P-T phase diagram.

The density anomaly arises in the model from a balance of two factors: the close-packed van der Waals contacts are pitted against more open hydrogen-bonded interactions. By tracking the average hydrogen-bond and van der Waals coordination of water molecules, we observe that hydrogen bond interactions are replaced with van der Waals contacts up to the temperature of maximum density (TMD). Beyond that temperature, both types of contacts decrease, due to increased thermal fluctuations that expand the fluid.

Finally, in the case of hydrophobic solute transfers, we find that the structure of water molecules in the first and second hydration shells is more temperature sensitive than the structure of bulk water. These trends contribute to the temperature dependence of the transfer thermodynamics that characterize hydrophobicity in the MB model.

Acknowledgments: KATS greatfully acknowledges support under a U.S. National Science Foundation Graduate Research Fellowship and a UCSF Regent's Fellowship. In Australia this research was supported by the Australian Research Council (ARC) (Grant No. A29530010), and SydCom the USyd/UTS Distributed Processing Facility

funded by an ARC infrastructure grant.

APPENDIX: Technical issue in NPT Monte Carlo Simulations

Typically in an NPT Monte Carlo simulation, constant pressure is achieved by allowing the volume of the box of molecules to fluctuate with an appropriately-weighted acceptance scheme[14]. Specifically, every R passes (1 pass = N molecules), an attempt is made to scale the dimensions of the box, and all of its component particles, according to:

$$q_i \rightarrow q_i(1 + \xi \Delta q) \tag{1}$$

where the q_is represent the particle coordinates and box length, and the random number ξ is generated over the interval $-1 \leq \xi_i \leq 1$, and Δq is a fixed maximum volume increment.

The frequency R with which volume-change attempts are made, and the maximum magnitude of those changes Δq are arbitrarily chosen. However, care should be taken in choosing these parameters. If volume-change attempts are too frequent and too large, the actual pressure (as calculated from the internal virial[14]) underestimates the target pressure by as much as 2%. Apparently, using such a protocol, the system is ripped apart before it ever attains its equilibrated state at the old volume. Hence, the system tends to be at a little higher energy and hence slightly expanded (i.e., at a lower pressure than desired).

The protocol suggested by Jorgensen[15] seems to work well for water-like particles. By such a scheme, volume-change attempts are made every 5 passes, and the maximum increment is adjusted to achieve a 50% acceptance ratio. In Figure 8 we compare the calculated pressure of MB water for several temperatures under this protocol at a reduced target pressure of 0.19, to a scheme in which volume-attempts are 5 times more frequent (i.e., every pass) and approximately 5 times as large.

References

[1] A. Ben-Naim, J. Chem. Phys., **59** (1973) 6535–6555.

[2] K.A.T. Silverstein, A.D.J. Haymet, and K.A. Dill, in preparation.

[3] A.D.J. Haymet, K.A.T. Silverstein, and K.A. Dill, International Symposium on Molecular Thermodynamics and Molecular Simulation, Tokyo, Japan, Jan 12-15, 1997, Hosei University, pp. 143–152.

[4] J.-P. Hansen and L. Verlet, Phys. Rev., **184** (1969) 151–161.

[5] F.H. Stillinger, Science, **209** (1980) 451–457.

[6] B. Lee, Biopolymers, **24** (1985) 813–823.

[7] B. Lee, Biopolymers, **31** (1991) 993–1008.

[8] A. Pohorille and L.R. Pratt, J. Am. Chem. Soc., **112** (1990) 5066–5074.

[9] L.R. Pratt and A. Pohorille, Proc. Natl. Acad. Sci. USA, **89** (1992) 2995–2999.

[10] W. Blokzijl and J.B.F.N. Engberts, Angew. Chem. Int. Ed. Engl., **32** (1993) 1545–1579.

[11] K.A. Dill, Science, **250** (1990) 297–298.

[12] A.D.J. Haymet, K.A.T. Silverstein, and K.A. Dill, Faraday Discussions, **103** (1996), in press.

[13] D.E. Smith and A.D.J. Haymet, J. Chem. Phys., **98** (1983) 6445–6454.

[14] M.P. Allen and D.J. Tildesley, Computer simulation of liquids, Oxford University Press, Oxford, 1987.

[15] W.L. Jorgensen, Chem. Phys. Lett., **92** (1982) 405–410.

FIGURE CAPTIONS

Figure 1: Rough sketch of the P-T phase diagram (log-log plot). The labels s, l, and g denote the solid, liquid, and gas phase regions respectively. Reduced temperature is normalized by the optimal hydrogen bond energy ($T^* = k_B T/\epsilon_{HB}$). Pressure is defined such that $P^* V^* = PV/\epsilon_{HB}$ (where $V^* = V/r_{HB}^2$).

Figure 2: Pair correlation function for pure MB water at four temperatures: T*=0.16 (solid), T*=0.20 (large-dashed), T*=0.24 (small-dashed), and T*=0.28 (dotted).

Figure 3: Average h-bond coordination of bulk water molecules vs. temperature using a cutoff of -0.5 (solid line) and -0.4 (dashed line).

Figure 4: Average vdw coordination of bulk water molecules vs. temperature using a cutoff of -0.06 (solid line) and -0.04 (dashed line).

Figure 5: Variance in the h-bond coordination of bulk water molecules vs. temperature (cutoff of -0.5).

Figure 6: water-water pair correlation function at four temperatures: (a) $T^* = 0.16$, (b) $T^* = 0.20$, (c) $T^* = 0.24$, and (d) $T^* = 0.28$ for shell (dashed) and bulk (solid) water molecules.

Figure 7: Angular distributions of neighboring water molecules around shell (dashed) and bulk (solid) water molecules at two temperatures: (a) first neighbors, $T^* = 0.16$; (b) second neighbors, $T^* = 0.16$; (c) first neighbors, $T^* = 0.24$; (d) second neighbors, $T^* = 0.24$.

Figure 8: Comparison of the calculated pressure from two volume-adjusting protocols as a function of temperature: $R = 1$ and $\Delta q = 0.1$ (diamonds) vs. $R = 5$ and $\Delta q \approx 0.02$ (pluses). The target pressure is $P^* = 0.19$.

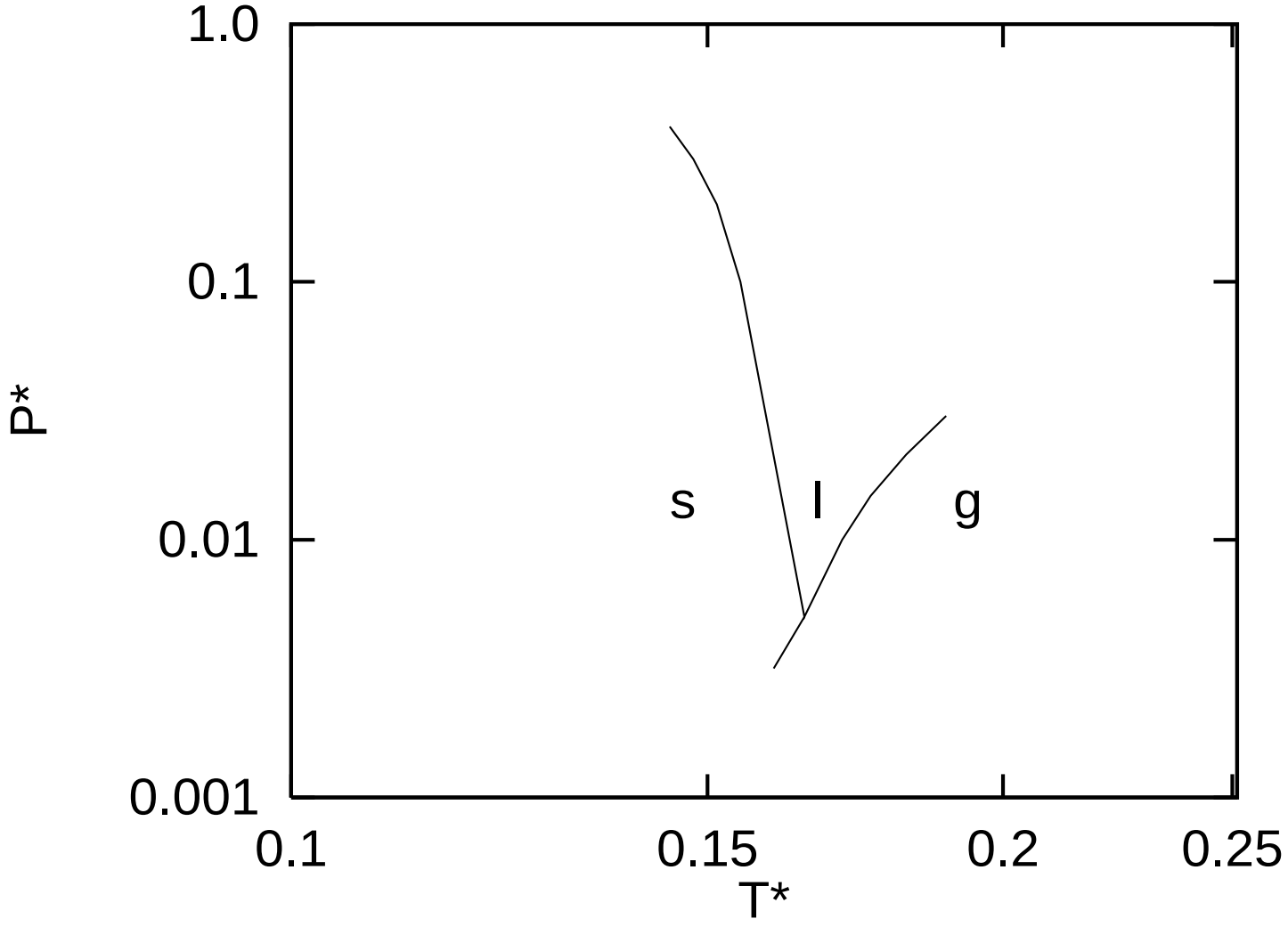
1.0
0.1
0.01
0.001
P*
s
l
g
0.1
0.15
0.2
0.25
T*

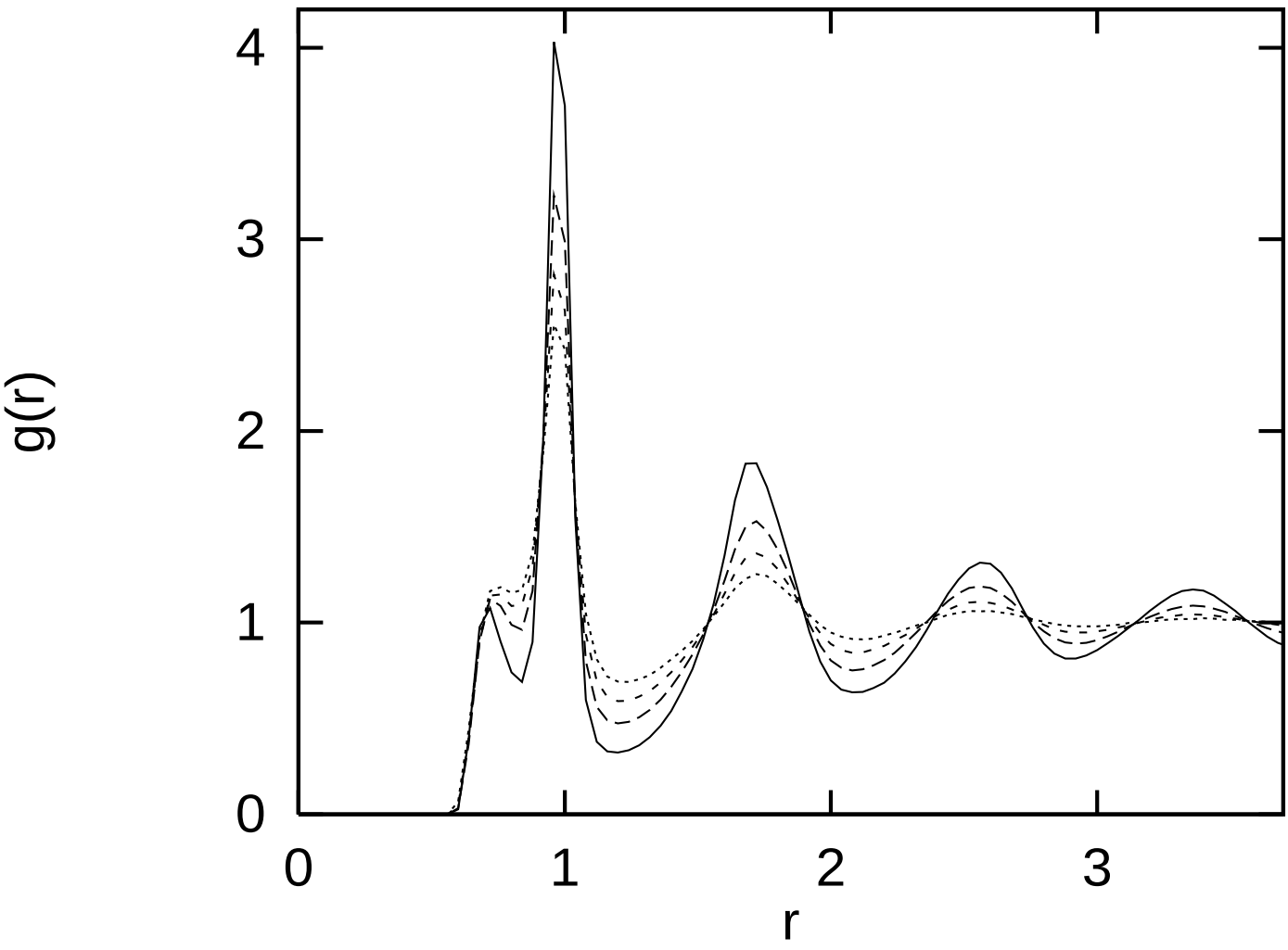
g(r)
4
3
2
1
0
0
1
2
3
r

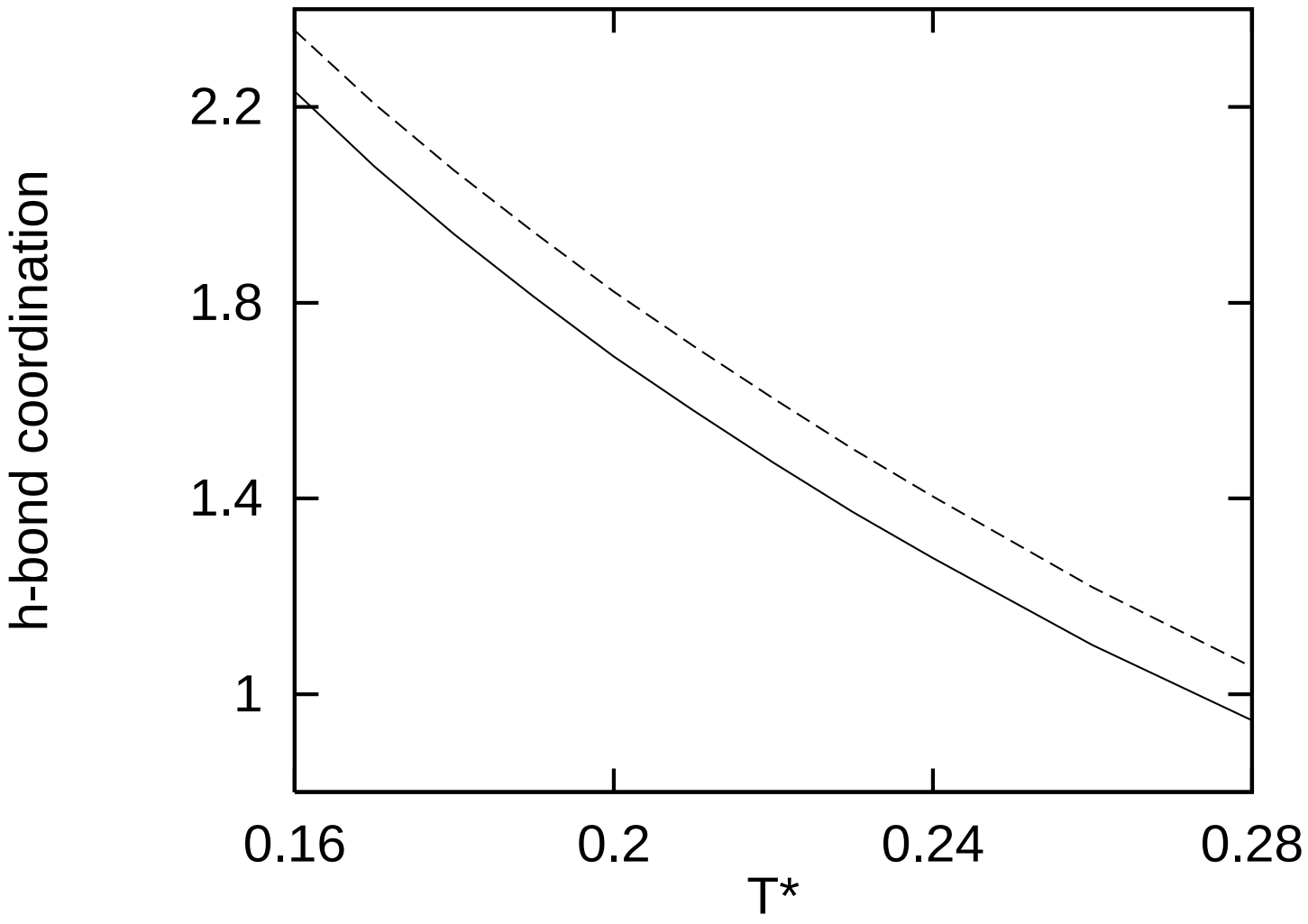
h-bond coordination
2.2
1.8
1.4
1
0.16
0.2
0.24
0.28
T*

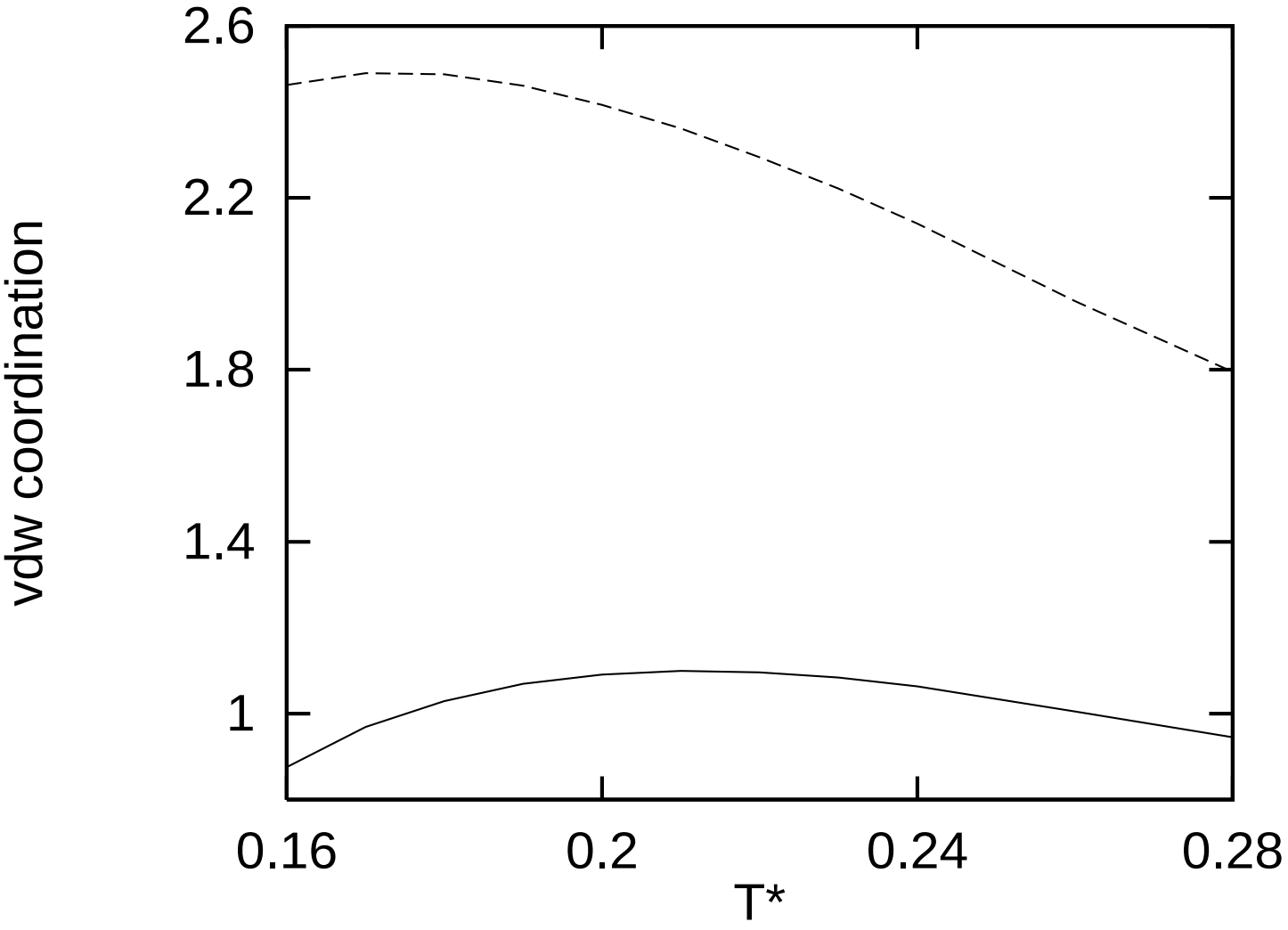
2.6
2.2
1.8
1.4
1
vdw coordination
0.16
0.2
0.24
0.28
T*

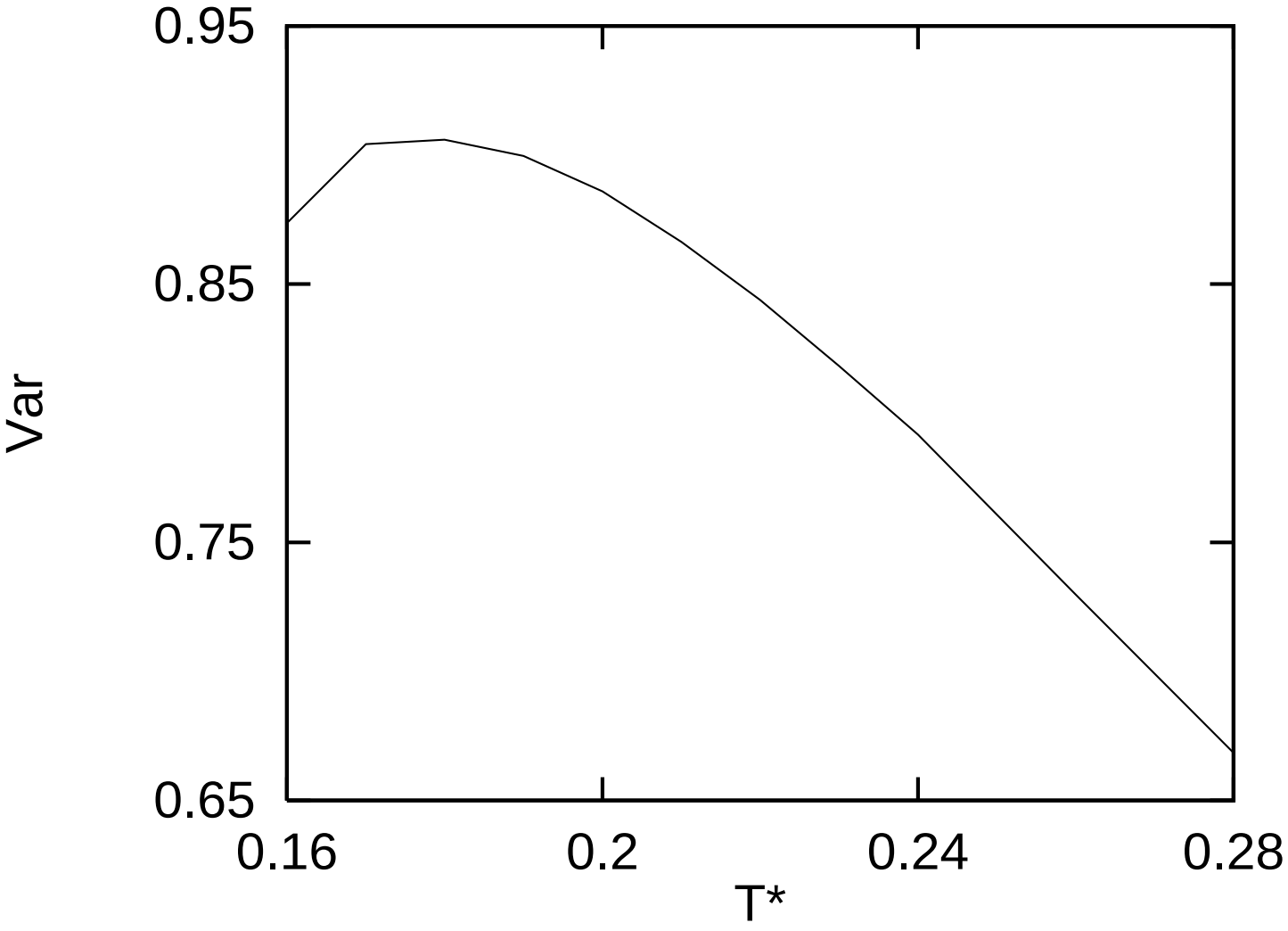
0.95
0.85
0.75
0.65
Var
0.16
0.2
0.24
0.28
T*

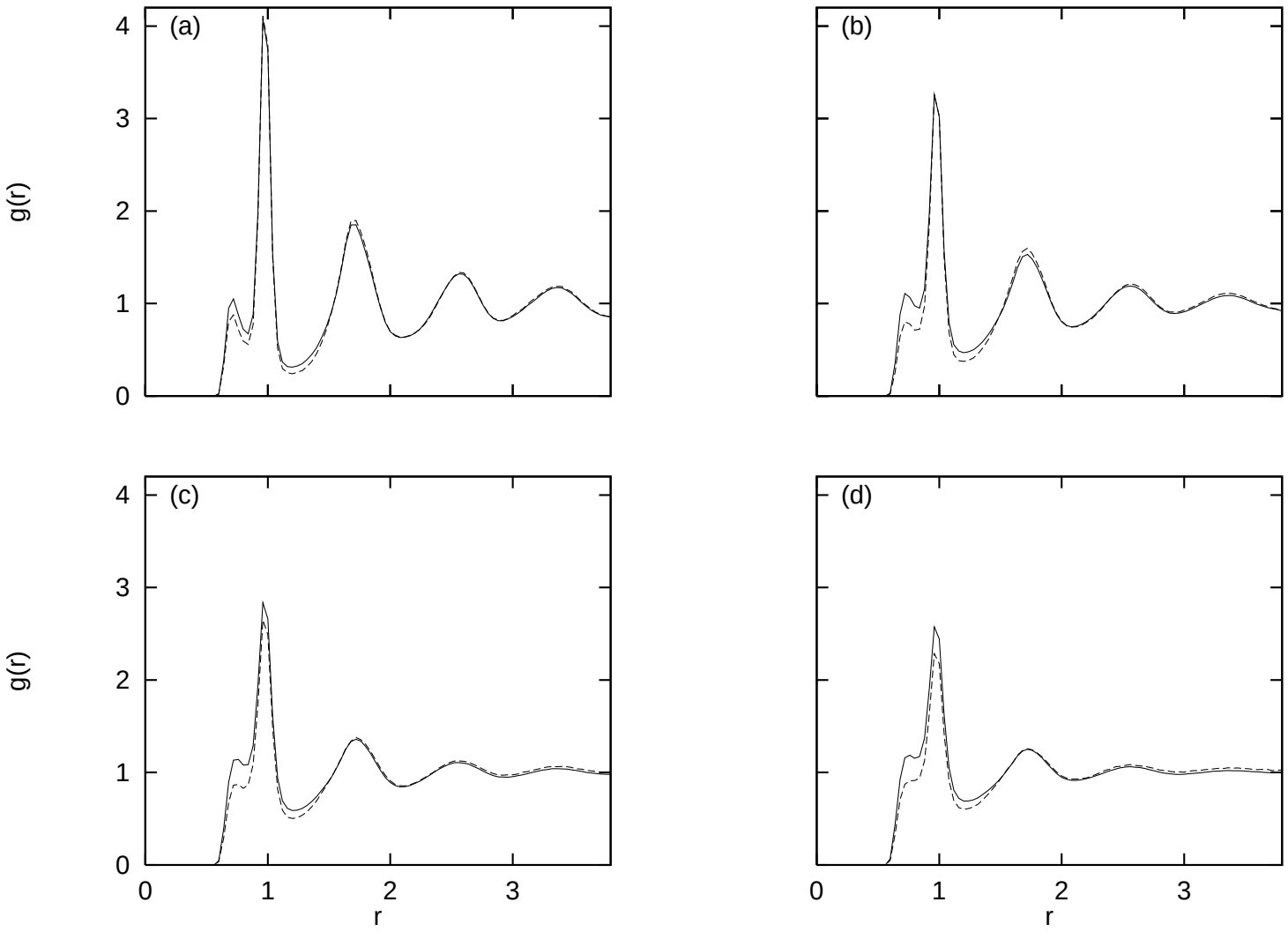
(a)
(b)
(c)
(d)
g(r)
g(r)
r
r
0
1
2
3
4

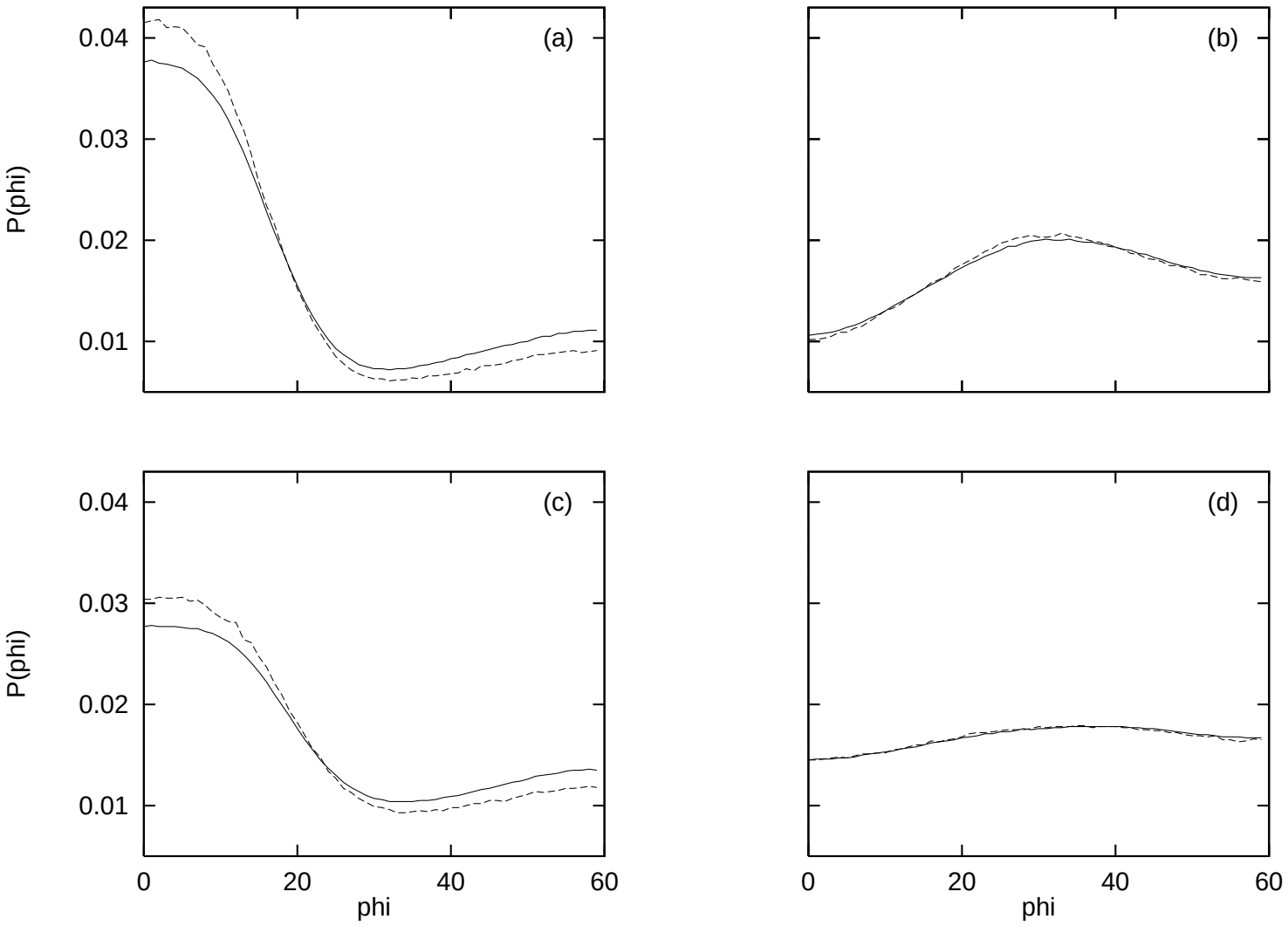
(a)
(b)
(c)
(d)
P(phi)
P(phi)
0.04
0.03
0.02
0.01
0.04
0.03
0.02
0.01
0
20
40
60
0
20
40
60
phi
phi

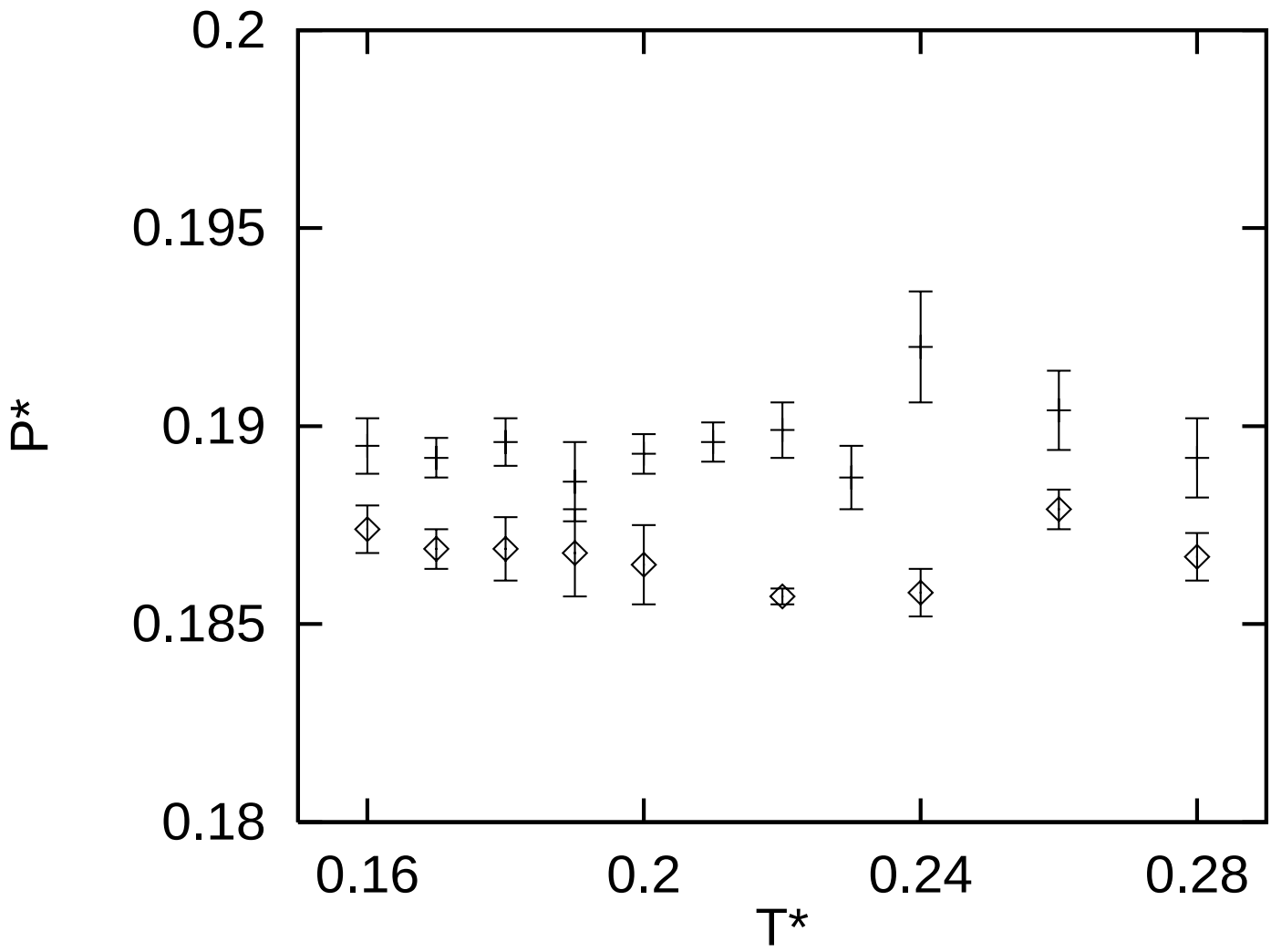
0.2
0.195
0.19
0.185
0.18
P*
0.16
0.2
0.24
0.28
T*